Astron. Astrophys. 352, L31–L35 (1999)

ASTRONOMY AND ASTROPHYSICS

LETTER

Letter to the Editor

A spectroscopic study of Be stars in the SMC cluster NGC 330⋆

W. Hummel[1], **T. Szeifert**[2,3], **W. Gässler**[1], **B. Muschielok**[1], **W. Seifert**[2], **I. Appenzeller**[2], **and G. Rupprecht**[4]

[1] Institut für Astronomie und Astrophysik und Universitätssternwarte München, Scheinerstrasse 1, D-81673 München, Germany
[2] Landessternwarte Heidelberg, Königsstuhl 12, D-69117 Heidelberg, Germamy
[3] ESO Santiago, Alonso de Cordova 3107, Casilla 19001, Santiago 19, Chile
[4] ESO, Karl-Schwarzschild-Strasse 2, D-85745 Garching, Germany

Received 12 August 1999 / Accepted 7 September 1999

Abstract. We present a spectroscopic study of early type emission line stars in the field of the young open SMC cluster NGC 330 which have been identified as Be stars by CCD imaging photometry by Grebel et al. (1992). 18 of the 20 program stars investigated can be confirmed to show Balmer emission lines superimposed on an early type spectrum. Two new Be stars in the field of NGC 330 have been detected. Hα emission equivalent width, FWHM and profile shapes (as far as resolved) do not differ from galactic Be stars, hence we suggest that rotation axis of Be stars in NGC 330 are not aligned, rather they are distributed randomly. Quantitative spectral analysis for Be40 and Be59 results in $T_{\rm eff} = 18\,000 \pm 1\,500\,K$, $\log g = 3.3 \pm 0.2$ and $T_{\rm eff} = 17\,000 \pm 1\,500\,K$, $\log g = 3.1 \pm 0.2$ respectively.

Key words: line: formation – line: profiles – radiative transfer – stars: circumstellar matter – stars: emission-line, Be

1. Introduction

About 10–20% of all galactic B-type stars with luminosity class III-V once showed Hα in emission and have therefore been classified as Be stars. The hydrogen, He I and singly ionized metallic emission lines originate in a circumstellar gaseous quasi-Keplerian disk. The formation of the rotating disk is associated with episodic mass-loss events, however the Be star mass-loss mechanism is not yet known. Low resolution (e.g. Dachs et al. 1986) as well as high resolution spectroscopy of individual emission lines (e.g. Hanuschik et al. 1998) has turned out to provide valuable information on the structure, kinematics and evolution of Be star circumstellar disks in the galaxy (Hummel & Hanuschik 1997).

The young open cluster NGC 330 in the SMC became a matter of interest, because of its high number fraction of Be stars (Be / (Be+B) $\simeq$ 50%; Feast 1972) and its low metallicity of $Z = 0.005$ (e.g. Hill 1999). Comparison between galactic Be stars and Be stars in the field of NGC 330 could play a key role in constraining the conditions for the Be phenomenon in general. Recently Grebel et al. (1992), Grebel (1995) and Keller et al. (1999) identified Be stars in NGC 330 by CCD imaging photometry using a Hα interference filter. Spectroscopic analyses of the brightest Be stars in NGC 330 with $V < 15\overset{\rm m}{.}8$ have been presented by Mazzali et al. (1996) and Keller & Bessell (1998).

In this study we present low resolution spectra of 20 photometrically identified Be stars in the field of NGC 330 with magnitudes down to $V = 18\overset{\rm m}{.}9$. The scientific aim is

- to verify photometrically identified Be stars by spectroscopy
- to classify Hα emission profile shapes
- and to determine stellar parameters

2. Observations and data reduction

The spectroscopic observations were collected in two nights with FORS1 in MOS mode at Antu on Paranal during commissioning 1. We collected photometrically identified Be stars from the list of Grebel (1995) and selected those Be stars for which a suitable MOS setup could be achieved. Magnitudes in the V-band range between 14–19 mag for the program stars. Since the FORS focal field ($6.8' \times 6.8'$) is larger than the field used by Grebel (1995), other resting MOS slits (mostly #14 – #18) were positioned on bright point sources for further instrument alignment tests. Spectra have been collected for more than 19 objects in each MOS focal field setup. The spectra of all targets have been considered, but in this study we only report on the results concerning emission line objects and early type stars.

The focal field setup and the setup for the telescope was prepared using a preliminary version of the FORS instrumental mask simulator. The nominal pointing was RA = 00:56:19.043, DEC = −72:27:59.81 for both instrument setups. Up to 7 reference stars were used to align the telescope pointing to the correct position. The optical distortion model of FORS1 was only applied to the first observation with a rotator angle of 0°, while it failed in our second run when testing alignments with

Send offprint requests to: W. Hummel

⋆ Based on observations collected during the commissioning 1 of FORS1 at ESO, VLT observatory, Paranal, Chile

Correspondence to: hummel@bigbang.usm.uni-muenchen.de

Table 1. Log of observations. From left to right: Julian date, date and UT at start of observation, FORS1 instrument modus, grism, filter and central wavelength, exposure time, approximative seeing and background counts per seconds and pixel in the corresponding alignment image.

JD	date	UT	mode	grism	filter	λ_c nm	time sec	seeing $''$	background c/s/p
2451083.34	27/09/98	06:26	IMG	none	none	[b]	0.25	0.8	80
2451088.28	02/10/98	06:43	MOS	600R	GG435	627	240	1.2	130
2451088.28	02/10/98	06:52	MOS	600B	none	462	360	1.2	130
2451091.34	05/10/98	08:08	MOS	600B	none	462	900	1.2	340
2451091.35	05/10/98	08:37	MOS	600R	GG435	627	600	1.2	340

Table 2. Target list and Hα emission line parameters. From left to right: name, V magnitude after Grebel (1995), name after Keller et al. (1999), FORS1-MOS slit number, coordinates, distance from the cluster center defined by the central point source at (RA = 00:56:18.8, DEC = $-$72:27:47.2), profile shape flag (s=single peak, d=double peak, a=asymmetric single peak), Hα emission equivalent width ($\Delta W_\alpha \simeq 10\%$), peak intensity (violet or central), red peak intensity, heliocentric radial velocities of peaks ($\Delta V \simeq 50 \mathrm{kms}^{-1}$) and FWHM.

name	V [mag]	KWB	MOS #	RA(2000) DEC(2000) hh:mm:ss.s dd:mm:ss.s	d $'$	p	W_α [Å]	I_V [I_c]	I_R [I_c]	V_V [km s^{-1}]	V_R [km s^{-1}]	FWHM [km s^{-1}]
Be109	18.609		3	00:56:01.7 -72:25:25.7	2.70	d	15	2.3:	2.9	129	333	411
Be 41	16.673	874	4	00:56:22.7 -72:25:47.4	1.02	s	35	5.3	—	194	—	334
Be 59	17.111	991	5	00:55:52.4 -72:26:03.5	2.65	s	34	6.0	—	196	—	263
Be 55	16.977	857	6	00:56:24.7 -72:26:24.8	1.43	s	48	5.7	—	232	—	404
Be 64	17.153	870	7	00:56:23.3 -72:26:50.6	1.00	d	1:	1.08	1.08	14	415	631
Be 68	17.307		8	00:55:48.9 -72:27:12.1	2.33	d	13	2.2	2.2	109	265	480
Be 1	14.408	80	9	00:56:06.7 -72:27:35.8	0.93	s	44	6.2	—	211	—	311
Be 4	15.350	215	10	00:56:23.0 -72:27:53.7	0.33	s	42	8.3	—	223	—	233
Be 78	17.466	2030	11	00:56:06.3 -72:28:19.0	1.08	d	24	2.9	2.7	59	335	548
Bal 224	[a]	485	11	00:56:06.5 -72:28:27.2	1.15	d	202	18.6	15.2	140	301	443
Be115	18.938		12	00:56:33.9 -72:28:43.6	1.48	s	7	2.0	—	186	—	315
F1e			17	00:56:28.1 -72:30:36.4	2.90	d	30	3.3	3.4	154	294	543
Be 40	14.408	1054	1	00:55:34.7 -72:29:12.2	3.62	a	36	3.9	—	289	—	539
Be 36	16.513	529	2	00:55:40.3 -72:26:41.0	3.10	s	40	5.5	—	183	—	357
Be 68			4			d	14	2.18	2.21	55	230	489
Be111	18.824		5	00:55:55.9 -72:25:20.4	3.00	-	0					
Be 9	15.562	258	6	00:56:00.0 -72:26:21.0	2.02	s	54	7.4	—	232	—	311
Be 96			8	00:56:09.1 -72:27:22.7	0.45	s	5	1.9	—	249	—	265
Be108	18.578		9	00:56:13.4 -72:28:53.4	1.12	-	0					
Be 77	17.456	1918	10	00:56:19.0 -72:28:22.1	0.58	d	11	2.0	1.8	69	315	526
Be 89	17.768		10	00:56:20.2 -72:28:21.5	0.58	s	51	5.7	—	181	—	425
Be 55			11			s	47	5.6	—	205	—	416
Be103	18.242		12	00:56:28.2 -72:28:33.0	1.03	a	19	2.6	—	92	—	512
F2e			12	00:56:28.8 -72:28:33.3	1.07	s	3:	2.4	—	186	—	197
Be 32	16.288	419	13	00:56:33.1 -72:27:05.0	1.28	s	27	5.3	—	144	—	242

[a] Not a Be star: #224 after Balona (1992) with $V \simeq 17\overset{\mathrm{m}}{.}1$; #515 after Sebo & Wood (1994) with $V \simeq 17\overset{\mathrm{m}}{.}4$

a rotator angle of 90°. Therefore stellar point sources were not exactly at the MOS slit center on our second night, in particular for slit positions at a large distance from the optical axis.

For the science and calibration exposures a common slit width of 1 arcsec is chosen for all MOS slits corresponding to 5 CCD pixels using the standard resolution collimator. This corresponds to $\Delta\lambda = 5.3$ Å. The wavelength range cover $3\,600$ Å $< \lambda < 7\,200$ Å for most of the targets. The exposure time was unique for all MOS slits. Each of the 19 MOS slits was 22 arcsec long, providing sufficient sky background. Some slits were occupied with two or more targets. The log of observations is given in Table 1.

The data reduction was performed using the MOS package as part of the ESO-MIDAS. The MOS standard reduction includes the subtraction of bias, normalized flat field correction, wavelength calibration, interactive specification of the sky background area in each MOS slit, flux calibration with the help of standard stars also obtained during commissioning 1, and correction for the heliocentric velocity.

3. Results

3.1. Astrometry

As with all frames obtained during commissioning 1 our preparation image also suffered from a numerical truncation error

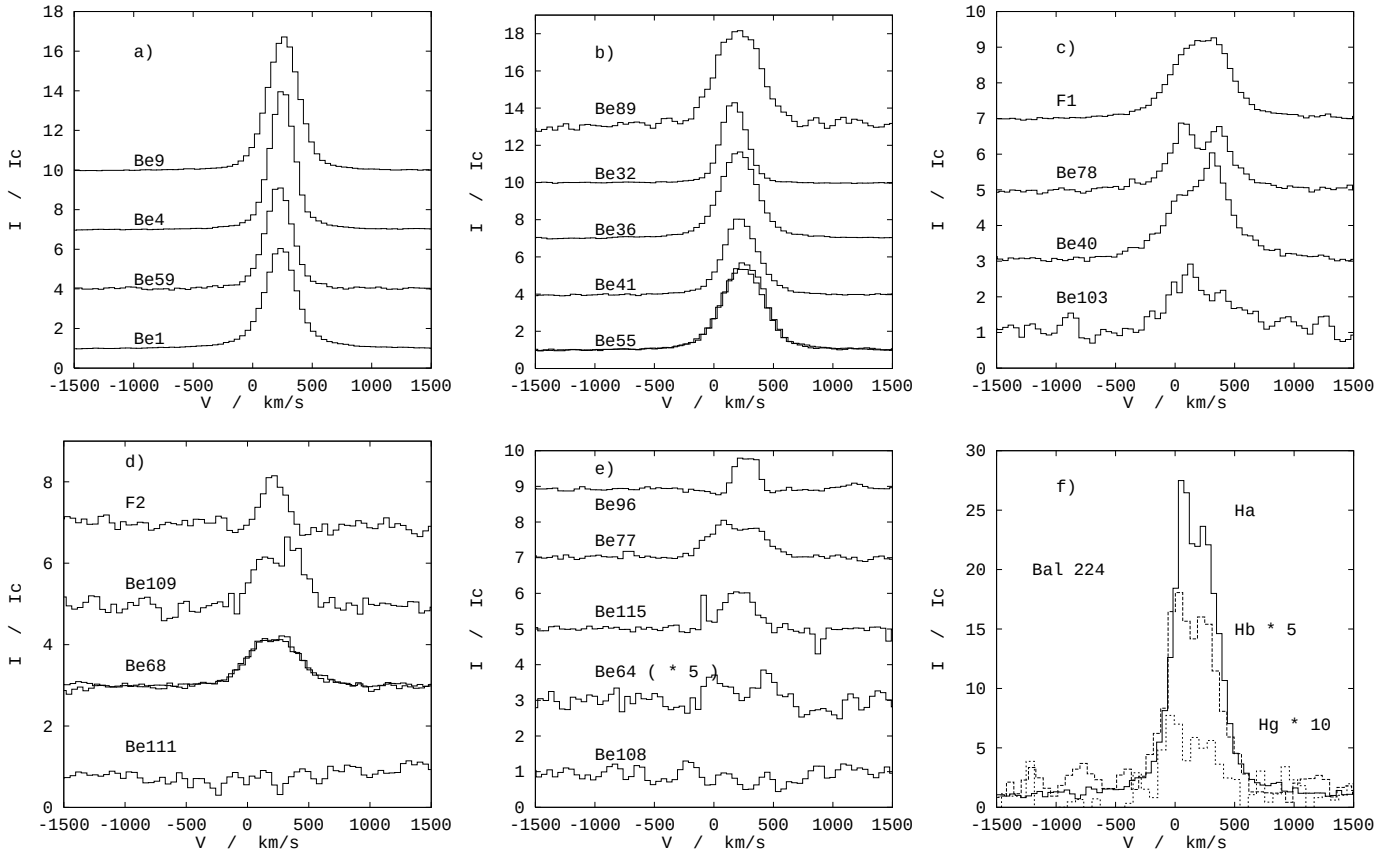

Fig. 1. a–e Hα emission line profiles of Be stars in the field of NGC 330. Profiles are normalized to the local stellar continuum. The abscissa gives the radial velocity scale in the heliocentric frame. **f** Hα, Hβ and Hγ of the irregular variable emission line object Bal 224.

with regard to the astrometric scale. We therefore compared the scale of our preparation image with scales of frames obtained during commissioning 2 and we have chosen a mean value of 5.546 $\times 10^{-5}$ °/pixel. The offset has been determined by comparing the optical positions with targets from the catalog of astrometric standards by Tucholke (1996). The mean position error is less than the seeing of 0.8″. The optical image distortion model of FORS1 is given by:

$$\Delta R = 3.458(-4)R - 1.178(-6)R^2 + 2.050(-9)R^3 \qquad (1)$$

for the standard resolution collimator and

$$\Delta R = 6.815(-4)R - 2.464(-6)R^2 + 8.540(-9)R^3 \qquad (2)$$

for the high resolution collimator where R is the observed distance in CCD-pixels from the optical axis, ΔR is the correction term in pixel units and $2.050(-9)$ stands for 2.050×10^{-9}. This correction (Eq. 1) has been taken into account by subtracting ΔR from R. The preparation image was observed at a zenith distance of $z \simeq 52°$, hence differential refraction amounted to less than 1 pixel at the rim of the image and was not corrected. Target coordinates are given in Table 2.

3.2. Hα spectroscopy

Target spectra of Hα are given in Fig. 1a–e and emission line parameters are summarized in Table 2. Among the 20 selected Be stars of Grebel (1995) 18 are confirmed to be emission line objects with an underlying early-type spectrum (see e.g. Figs. 3,4). The absence of strong forbidden low excitation emission lines [O I] and [Fe II] typical for B[e] stars support the identification as classical Be stars (Allen & Swings 1976). Two of the fainter targets (Be108 and Be111) lack emission in Hα although they have been identified as Be stars with larger (R-Hα) index than e.g. Be115 by Grebel (1995). Two targets have been observed twice (Be 68 and Be55) and no variability was detected on the timescale of weeks.

Two new Be stars (F1 and F2) have been detected in the field of NGC 330. F1 is out of the field studied by Grebel (1995) and appears at the southern rim of Keller et al. (1999). F2 is close to Be103 and has not been identified as an Hα emission line object by Keller et al. (1999) or Grebel (1995).

Hα emission strengths and line shapes are very similar to those of galactic Be stars, in particular when compared with surveys of similar spectroscopic resolution (e.g. Dachs et al. 1986). A simple preliminary classification is given in Table 2.

Measured FWHM of Hα emission range from 630 km s^{-1} (Be64) to 200 km s^{-1} (F2). Note that the FWHM of the instrumental profile of 5.3 Å corresponds to 234 km s^{-1}.

Several targets (Be78, Be89, Be77 and Be108) appear as close visual double stars on the preparation image. The resulting

Table 3. Best fit stellar parameters of two Be stars

name	V	$v \sin i$	$T_{\rm eff}$	$\log g$
Be40	14.41	–	18 000±1 500	3.3±0.2
Be59	17.11	150	17 000±1 500	3.1±0.2

Hα emission equivalent widths are therefore considered to be lower limits.

3.3. Radial velocities

We derived a mean value of the Hα radial emission peak velocity using the $V_{\rm V}$ values from Table 2 of those stars indicated as 's' but also included the mean value of the symmetric double peaks from Be68 (2 times) and Be78. We find $V_\alpha = +176\,{\rm km\,s^{-1}}$ with $\sigma_\alpha = 28\,{\rm km\,s^{-1}}$. This value is slightly larger than the systemic radial velocity of NGC 330 $V_{330} = +146\,{\rm km\,s^{-1}}$ (Feast & Black 1980).

3.4. The peculiar emission line object Bal 224

Bal 224 is known to be photometrically variable in the V-band (Balona 1992; Sebo & Wood 1994). The spectrum of Bal 224 shows only three strong Balmer lines in emission (Fig. 1f) with an extremely steep decrement of Hα/Hβ=7.1 and Hγ/Hβ=0.21, but the faint continuum is flat and featureless. From the steep Balmer decrement and the lack of He I emission we suggest a cool gas with $T \ll 5\,000$ K. The asymmetric double peaks most probably originate from an accretion disk. However a re-investigation is required to clarify the nature of this object.

4. Quantitative spectral analysis of Be40 and Be59

Though the observations suffer from low resolution and low S/N we fit model atmospheres to several He I and Balmer absorption lines. The lack of He II absorption lines in the observations is consistent with spectral types later than B2, the lack of Mg II indicates a spectral type earlier than B8 (Steele et al. 1999). For the profile fits we follow mostly the method described by Becker & Butler (1990) but use the extended model atmosphere grid of Vrancken et al. (1996) to construct the lines of constant equivalent width in the $\log g - T_{\rm eff}$ diagram. Since there are no He II profiles which can be used to constrain the stellar parameters we additionally calculate χ^2 for each model profile fit as a cross-check. For Be40 only Hδ is affected by fill-in emission, hence Hϵ is used for the model constraint (Fig. 2). For Be59 both Hδ and Hϵ are affected by fill-in emission (Fig. 4), hence only the wings of the Balmer absorption lines have been used to constrain the model fit. The difference between model fit and observation is given as net emission in Figs. 3 and 4. The best-fit model parameters of both stars are given in Table 3.

5. Conclusions

The Hα emission line parameter statistics of our sample agrees with that of Keller & Bessell (1998) but differs in two ways

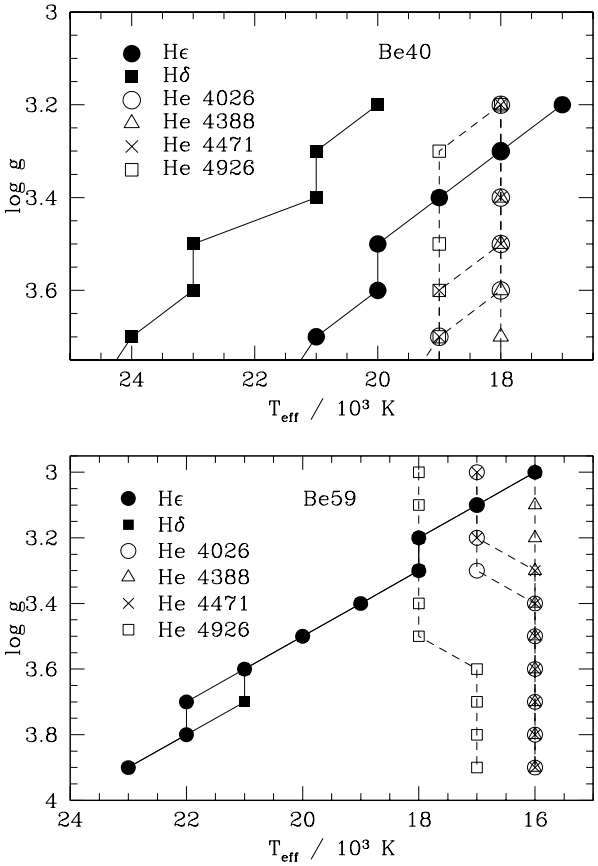

Fig. 2. Lines of constant equivalent widths in the $\log g$ - $T_{\rm eff}$ diagram for several hydrogen and He I absorption lines. Upper for Be40 without rotational broadening; Lower for Be59 with $v \sin i = 150\,{\rm km\,s^{-1}}$.

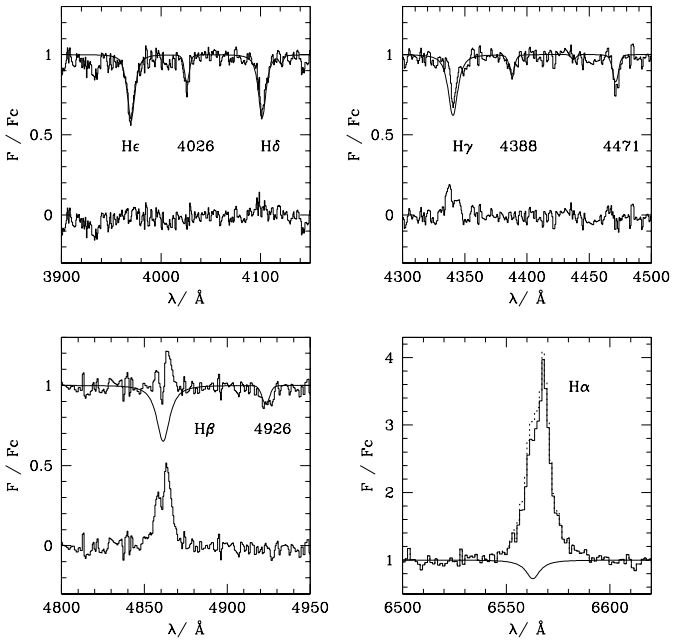

Fig. 3. Selected wavelength regions of the observed spectrum and best fit model spectrum of Be40 (upper part) and the difference (lower part), showing the net emission due to the circumstellar disk. The dotted Hα profile is corrected for stellar absorption.

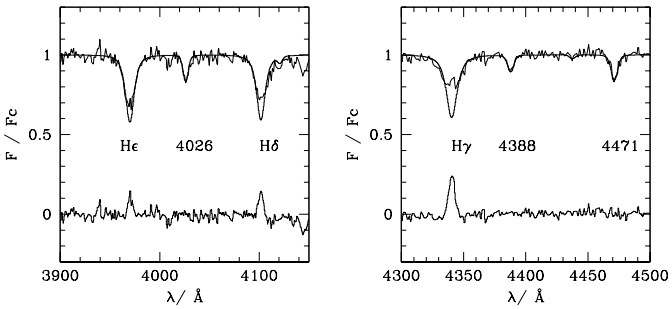

Fig. 4. As Fig. 3, except for Be59.

from that of Mazzali et al. (1996). We find no correlation between the FWHM and the equivalent width of Hα emission lines (see Table 2). The second observational fact is that *there are* indeed double peak Hα emission lines in NGC 330 with equivalent widths ranging from very small (Be64) up to 24 Å (Be78). In particular the first finding is difficult to explain for a sample of Be star disks with aligned rotation axes as proposed by Mazzali et al. (1996). Since the Hα emission equivalent width mostly reflects the size of the circumstellar disk, the lower mean kinematical broadening in large Keplerian disks would result in lower FWHM for stronger Hα lines if $v \sin i$ is kept constant (e.g. Hanuschik 1988, his Fig. 1a). This relation is not found in our sample, hence we conclude that $v \sin i$ is not a constant, rather the rotation axis of Be stars in NGC 330 are distributed randomly. Our findings fully confirm the results of Keller & Bessell (1998) who came to the same conclusion.

Acknowledgements. We thank K. Butler for helpful comments on the profile fits. The funding through "Verbundforschung Astronomie" by the Bundesminister für Forschung und Bildung under grants 053MU104, 053GO10A and 053HD50A is gratefully acknowledged.

References

Allen, D.A., Swings, J.P., 1976, A&A 47, 203
Arp, H., 1959, AJ 64, 245
Balona, L.A., 1992, MNRAS 256, 425
Becker, S., Butler, K., 1990, A&A 235, 326
Dachs, J., Hanuschik, R., Kaiser, D., Rohe, D., 1986, A&A 159, 276
Feast, M.W., 1972, MNRAS 159, 113
Feast, M.W., Black, C., 1980, MNRAS 191, 285
Grebel, E.K., 1995, PhD, University Bonn
Grebel, E.K., Richtler, T., de Boer, K.S., 1992, A&A 254, L5
Hanuschik, R.W., 1988, A&A, 190, 187
Hanuschik, R.W., Hummel, W., Sutorius, E., Dietle, O., Thimm, G., 1996, A&AS 116, 309
Hill, V., 1999, A&A 345, 430
Hummel, W., Hanuschik, R.W., 1997, A&A 320, 852
Keller, S.C., Bessell, M.S., 1998, A&A 340, 397
Keller, S.C., Wood, P.R., Bessell, M.S., 1999, A&AS 134, 489
Mazzali, P.A., Lennon, D.J., Pasian, F., Marconi, G., Baade, D., Castellani, V., 1996, A&A 316, 173
Sebo, K.M., Wood, P.R., 1994, AJ 108, 932
Steele, L.A., Negueruela, I., Clark, J.S., 1999, A&AS 137, 147
Tucholke, H.J., de Boer, K.S., Seitter, W., 1996, A&AS 119, 91
Vrancken, M., Butler, K., Becker, S., 1996, A&A 311, 661